Recognition of the T Stem−Loop of a Pre-tRNA Substrate by the Ribozyme from *Bacillus subtilis* Ribonuclease P†

Andrew Loria and Tao Pan*

Department of Biochemistry and Molecular Biology, University of Chicago, Chicago, Illinois 60637

Received January 21, 1997; Revised Manuscript Received March 27, 1997⊗

ABSTRACT: The ribozyme from bacterial ribonuclease P (denoted P RNA) specifically recognizes the coaxially stacked T stem−loop and the acceptor stem of a tRNA substrate. This recognition is mediated primarily through tertiary interactions. At least four 2′-OH groups in the T stem−loop region have been implicated as direct contacts with *Bacillus subtilis* P RNA [Pan, T., et al. (1995) *Proc. Natl. Acad. Sci. U.S.A. 92*, 12510]. Effects of six single 2′-OH → 2′-H substitutions and two base mutants of the G19−C56 tertiary interaction in tRNA on substrate binding (K_d) and the chemical step of the reaction (k_2) have been determined using a $tRNA^{Phe}$ substrate containing a 2′-deoxy residue at the cleavage site. Our results show that at least five functional groups in the T stem−loop of tRNA directly participate in P RNA binding. They include the 2′-OH groups of residues 54, 56, 61, and 62 and possibly the 4-amino group of the conserved C56. The 2′-OHs of residues 54, 61, and 62 are positioned within the same minor groove due to stacking of the reverse Hoogsteen U54-A58 pair on the G53-C61 Watson−Crick pair in the T stem. This groove is extended to the 4-amino group of C56 through the tertiary structure of tRNA. We use the term "tertiary groove" to describe alignment of functional groups through tertiary folding of an RNA. The binding also includes the 2′-OH of nucleotide C56 which is not located in this tertiary groove. Assuming additivity, these five interactions can contribute 7.4 kcal/mol or 10^5-fold in binding but only −0.5 kcal/mol or ∼2-fold in chemistry at 37 °C. The P RNA binding site for the T stem−loop includes at least the previously identified A230 as well as the A130 in *B. subtilis* P RNA. The K_d and k_2 data from the A130G mutant of *B. subtilis* P RNA suggest that A130 may be proximal to residue 56 in tRNA. These results show how the highly structured T stem−loop region in a pre-tRNA substrate is bound by the *B. subtilis* P RNA. This is among the first examples of how a nonhelical RNA structure can be recognized by another RNA through tertiary interactions.

An RNA molecule can specifically recognize another RNA in two ways: sequence recognition in which two RNAs associate through Watson−Crick base pairs and structural recognition involving tertiary interactions. The *Tetrahymena* group I intron ribozyme utilizes both modes of recognition for substrate binding (Cech, 1993). Initially, five Watson−Crick base pairs and one G-U wobble pair form between the substrate and the internal guide sequence of the ribozyme, resulting in an intermolecular RNA helix, P1. The P1 helix is then docked into the catalytic core of the ribozyme. This docking step involves the formation of tertiary interactions with at least four functional groups in P1: three specific 2′-OH groups and the 2-amino group of the G-U wobble pair, all within the structural context of an A-form helix (Strobel & Cech, 1993, 1995). Thus, the *Tetrahymena* ribozyme can be viewed as being capable of recognizing the structure of RNA helices. Indeed, group I intron ribozyme constructs designed with the substrate P1 helix in *trans* can efficiently and accurately carry out the transesterification reaction (Doudna & Szostak, 1989; Doudna & Cech, 1995).

Another large ribozyme capable of structural recognition of its RNA substrate is the catalytic RNA component from bacterial ribonuclease P. Bacterial RNase P is composed of one 330−420 nucleotide RNA and a 13−15 kDa protein [reviewed by Altman et al. (1993) and Pace and Brown (1995)]. RNase P is responsible for producing the mature 5′ end of all tRNAs *in vivo* through a specific endonucleolytic cleavage of tRNA precursors. The RNA component (denoted P RNA) alone can carry out all RNase P functions *in vitro* (Guerrier-Takada et al., 1983). The coaxially stacked acceptor stem and the T stem−loop structure of the tRNA substrate are the major determinants for recognition by P RNA (McClain et al., 1987; Kahle et al., 1990; Thurlow et al., 1991). P RNA contains two independently folding domains which appear to directly contact distinct regions of this tRNA structure (Pan & Jakacka, 1996; Loria & Pan, 1996). Folding domain I is mainly involved in binding of the T stem−loop, whereas folding domain II binds the acceptor stem around the cleavage site and the 3′-CCA in tRNA. The P RNA−tRNA interaction appears to be mostly mediated through tertiary interactions. Only the 3′-CCA sequence in tRNA may form Watson−Crick base pairs with two guanosine residues in a loop region in P RNA (Kirsebom & Svard, 1994; LaGrandeur et al., 1994; Oh & Pace, 1994).

Potential 2′-OH groups involved in direct contacts with P RNA have been previously identified through circular permutation analysis coupled with dephosphorylation (CPA-DP; Pan et al., 1995). In this experiment, a 2′-OH group is converted to a 2′,3′-cyclic phosphate in the context of a circularly permuted (CP) molecule. This conversion changes the 2′-OH from a potential hydrogen bond donor to a

† This work was supported by grants from the NIH (GM52993) and the American Cancer Society (JFRA-543).

* Corresponding author. Telephone: (773) 702-4179. Fax: (773) 702-0439. E-mail: taopan@midway.uchicago.edu.

⊗ Abstract published in *Advance ACS Abstracts,* May 15, 1997.

S0006-2960(97)00115-3 CCC: $14.00

hydrogen bond acceptor. If a 2′-OH group functions as a hydrogen bond donor to P RNA, a decrease in the cleavage efficiency of its corresponding CP isomer would be observed. Upon removal of the 2′,3′-cyclic phosphate, the 2′-OH is again available as a hydrogen bond donor. The dephosphorylated CP isomer may show increased cleavage efficiency compared to the CP isomer containing a 2′,3′-cyclic phosphate. Using this method, four 2′-OH groups at nucleotides 54, 57, 61, and 62 in tRNA were identified as potential candidates for contacting P RNA (Pan et al., 1995). Further characterization indicated that the 2′-OH of nucleotide 62 in tRNA interacts with the conserved A230 residue in *Bacillus subtilis* P RNA (Pan et al., 1995). Furthermore, four other 2′-OH groups within this region, 53, 55, 56, and 18, also showed a strong decrease in cleavage efficiency of their corresponding CP isomers. However, no increase in activity was observed upon removal of the cyclic phosphate for this group, suggesting that the initial decrease in cleavage efficiency of these CP isomers may be due to misfolding, loss of direct contacts that cannot be restored in the context of dephosphorylated CP isomers, or both. Thus, eight 2′-OH groups in the T stem−loop region are candidates for direct contacts with P RNA.

This paper describes determination of thermodynamic parameters of tRNA substrates containing a single functional group substitution (e.g. 2′-OH → 2′-H). An assay is developed in which the effects on the substrate binding constant (K_d) and on the chemical step (k_2) of these substitutions can be measured directly. Using the CPA-DP results as a guideline, six 2′-OH groups were analyzed, four of which were shown to contribute significantly to binding to *B. subtilis* P RNA. In addition, the 4-amino group of the conserved nucleotide C56 was also implicated in direct contact with P RNA. Thus, the major determinants of T stem−loop recognition are four functional groups aligned within a groove dictated by the tertiary structure of tRNA. The fifth group points to a different surface in tRNA also involved in P RNA recognition.

MATERIALS AND METHODS

Preparation of the Modified tRNA Substrates. All RNA fragments without modifications were obtained by *in vitro* transcription using T7 RNA polymerase (Milligan et al., 1987). All oligoribonucleotides containing a single 2′-OH → 2′-H substitution were synthesized by phosphoramidite chemistry using standard protecting groups (amidites purchased from PerSeptive Biosystems, Cambridge, MA) or using novel protecting groups (Scaringe, 1996; oligoribonucleotides custom synthesized by Dharmacon Research, Boulder, CO). tRNA substrates were obtained by ligating a synthetic oligoribonucleotide to another RNA using T4 DNA ligase and a deoxyoligonucleotide splint (Moore & Sharp, 1992). The sequence of the "wild-type" tRNA substrate with a single deoxyribonucleotide at the cleavage site is 5′-CGCUdC (dC for deoxy-C) followed by the sequence of yeast $tRNA^{Phe}$ (Figure 1). This substrate was synthesized by ligating a synthetic oligoribonucleotide, 5′-CGCUd-CGCGGAUUUA (14mer), to an RNA transcript containing nucleotides 10−76 of yeast $tRNA^{Phe}$ [YF(10−76)]. A typical ligation reaction mixture contained 10 pmol of 5′ ^{32}P-labeled 14mer, 25 pmol of YF(10−76), 25 pmol of DNA splint of the sequence 5′-CTCCCAACTGAGCTAAATCCGCGAGCG, 50 mM Tris-HCl (pH 7.6), 10 mM $MgCl_2$, 10 mM β-mercaptoethanol, and 1 unit/μL T4 DNA ligase (U.S. Biochemicals, Arlington Heights, IL) at 16 °C for 16−20 h. The yield of this particular ligation reaction was quantitative.

Two ligation steps were required to make tRNA substrates with two modifications. In general, the first ligation reaction produced YF(10−76) containing a single 2′-OH → 2′-H substitution. For example, the substrate containing 2′-deoxy nucleotides at positions −1 and 54 was prepared by ligating an oligoribonucleotide, 5′-GdUUCGAUCCACAGAAUUCG-CACCA, to an RNA transcript containing nucleotides 10−52 of yeast $tRNA^{Phe}$ [YF(10−52)] in the presence of the DNA splint, 5′-CTGTGGATCGAACACAGGACCTCCA-GATC. The ligation product, YF(10−76)+d54, was then purified by denaturing gel electrophoresis and used for the next ligation reaction with the 14mer described above.

Kinetics of the Cleavage Reaction. All kinetic measurements were carried out under single-turnover conditions with a 10−10000-fold molar excess of P RNA over 5′ ^{32}P-labeled substrates. The ribozymes and the substrates were renatured separately by heating in buffer at 85−90 °C for 2 min, followed by incubation at room temperature for 3 min. $MgCl_2$ was then added and the ribozyme incubated for 10 min at 50 °C. The substrate was incubated for 5 min at room temperature; KCl was then added followed by incubation for 5 min at 37 °C. The reaction was initiated by mixing the ribozyme and the substrate solutions in equal volumes. At specific times, aliquots were removed and the reaction was quenched by mixing with 2 volumes of 9 M urea/50 mM EDTA. Most reactions were performed in 50 mM Tris-HCl (pH 7.8, at 37 °C), 100 mM $MgCl_2$, and 0.6 M KCl at 37 °C. The radioactive substrate and product were separated using polyacrylamide gels containing 7 M urea and quantitated using a Phosphorimager (Fuji Medicals, Stamford, CT). Reaction rates were obtained by plotting the amount of remaining substrate over time and fitting the curve to a single-exponential decay using Kaleidagraph. To obtain k_2 and K_d, the reaction rates were plotted as a function of ribozyme concentration and the curve was fitted using Kaleidagraph with the equation

$$\text{rate} = k_2[\text{P RNA}]/(K_d + [\text{P RNA}])$$

where k_2 is the chemical step and K_d is the dissociation constant of the ES complex. The K_d and k_2 values were obtained at eight different P RNA concentrations. In general, the K_d and k_2 values determined from two independent experiments differed by a factor of $\leq$1.25.

Cloning of P RNA and tRNA Mutants. The P RNA variant containing the A230G mutation was cloned previously for the CPA-DP experiment (Pan et al., 1995). The A130G mutants were obtained by subcloning a fragment of *B. subtilis* P RNA from the *Bam*HI (5′ end of P RNA) to the *Bbs*I site (nucleotides 143 and 144). A DNA oligonucleotide, 5′-A T C C G A A G A C G T A G G C T T T T T T C C T G C-CGVCAGCCTCTAAAGA (V = C, G, or A), and the T7 promoter sequence were used as primers for PCR. The reaction products were cut with restriction enzymes *Bam*HI and *Bbs*I. Individual clones were sequenced, and all three mutants, A130G (g130), A130C, and A130U, were isolated. The tRNA plasmid encoding the G19C/C56G mutant of yeast $tRNA^{Phe}$ (c19g56) was kindly provided by O. Uhlenbeck (University of Colorado, Boulder, CO). The plasmid DNA encoding the G19A/C56U mutant of yeast $tRNA^{Phe}$ (a19u56)

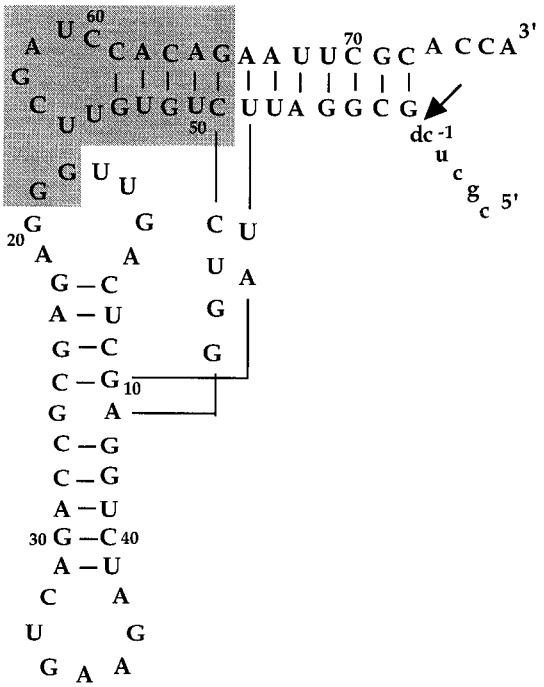

FIGURE 1: Sequence of the tRNA^{Phe} substrate used in this study. The cleavage site is indicated by an arrow, and nucleotides 5′ to it are shown in lowercase. dC at residue −1 represents the 2′-deoxynucleotide at the cleavage site. The T stem−loop region of interest in this study is shaded. This region includes the T stem−loop (residues 49−65) and the two D loop nucleotides (18 and 19) that interact with the T loop in the tertiary structure of tRNA.

was cloned by PCR amplification of the wild-type yeast tRNA^{Phe} template using primers containing appropriate mutations.

RESULTS

Kinetic Analysis of the Pre-tRNA^{Phe} Substrate with a 2′-OH → 2′-H Substitution at the Cleavage Site. In order to determine the effects of site-specific modifications on substrate binding and the chemical step of the P RNA reaction, a tRNA^{Phe} substrate was designed to contain a single 2′-deoxynucleotide at the cleavage site (Figure 1). This substrate is composed of five nucleotides 5′ to the cleavage site plus the mature yeast tRNA^{Phe} sequence. Cleavage rates under single-turnover conditions ([E] >> [S]) were measured at increasing concentrations of *B. subtilis* P RNA. At 37 °C and pH 7.8 with 100 mM $MgCl_2$ and 0.6 M KCl, this reaction was saturable, and the rates could be fit to a simple two-component curve with a maximum rate (v_{max}) of 0.67 min^{-1} and a K_m value of 0.10 μM (Figure 2A). At constant Mg^{2+} and K^+ concentrations, v_{max} shows a logarithmic linear dependence on pH with a slope of ∼1.1 (Figure 2B). This strong pH dependence suggests that v_{max} reflects the chemical step (k_2). For the *B. subtilis* P RNA, the bimolecular on-rate (k_1) and the dissociation rate (k_{-1}) of a *B. subtilis* tRNA^{Asp} substrate at pH 8.0 with 100 mM $MgCl_2$ and 0.8 M NH_4Cl have been determined to be 3.6×10^8 M^{-1} min^{-1} and 39 min^{-1}, respectively (Beebe & Fierke, 1994). Under our experimental conditions where [E] ≥ 10[S], K_m equals $(k_{-1} + k_2)/k_1$. If the k_{-1} for our tRNA^{Phe} substrate is comparable to that of tRNA^{Asp}, then k_{-1} >> k_2 and K_m reduces to k_{-1}/k_1, or K_d. Consistent with this assumption, the K_d value of 0.10 μM determined for our tRNA^{Phe} substrate

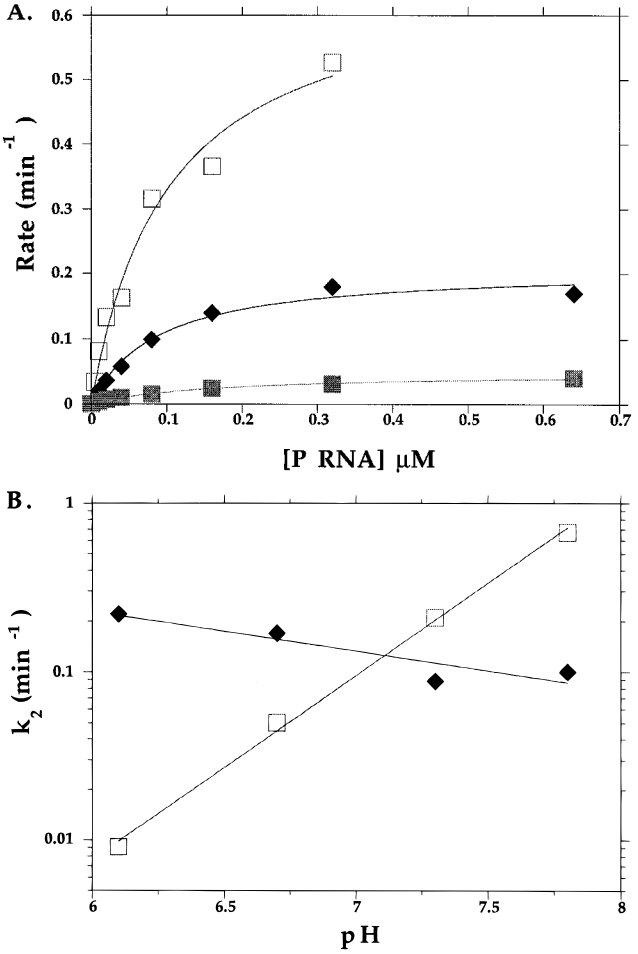

FIGURE 2: (A) Dependence of reaction rates on *B. subtilis* P RNA concentration. The tRNA^{Phe} substrate contains a single 2′-deoxynucleotide at the cleavage site. Rate dependence is shown for pH 7.8 (□), pH 7.3 (◆), and pH 6.7 (■). (B) Dependence of the chemical step (k_2, □) and binding constant (K_d, ◆) of the tRNA^{Phe} substrate on pH. The pH dependence of log(k_2) has a slope of 1.09, corresponding to a factor of 71 from pH 6.1 to 7.8. The pH dependence of log(K_d) has a slope of −0.2, corresponding to a factor of 2 from pH 6.1 to 7.8.

is remarkably close to that calculated for the tRNA^{Asp} substrate using the microscopic rate constants (0.11 μM).

The assumptions that $v_{max} = k_2$ and $K_m \approx K_d$ for the modified tRNA^{Phe} substrate are plausible on the basis of the ribozyme literature. Smith and Pace (1993) have constructed a tRNA^{Phe} substrate with a single nucleotide 5′ to the cleavage site. This 5′ residue was a deoxynucleotide representing a 2′-OH → 2′-H substitution at the cleavage site. The v_{max} of this substrate with *Escherichia coli* P RNA was also pH-dependent and was interpreted as the rate of the chemical step of the reaction. In the case of the *Tetrahymena* group I ribozyme (Herschlag et al., 1993), a single deoxynucleotide substitution at the cleavage site reduced the chemical step by a factor similar to that observed for P RNA-catalyzed cleavage of our tRNA^{Phe} substrate. P RNA is believed to recognize the structure of all tRNA substrates in a similar fashion (Westhof & Altman, 1994; Harris et al., 1994). For the *B. subtilis* P RNA, k_1 for a tRNA^{Phe} substrate and the dissociation constant of its tRNA product (k_3) at 100 mM $MgCl_2$ and 1 M KCl have been estimated to be ∼2.1×10^8 M^{-1} min^{-1} and 1−3 min^{-1}, respectively (A. Loria and T. Pan, unpublished results). Both values are within 2-fold of those for tRNA^{Asp} [3.6×10^8

Table 1: Dependence of k_2 and K_d on the Ionic Conditions

ionic conditions	K_d (μM)	k_2 (min^{-1})
100 mM $MgCl_2$	6.4 ± 1.0	0.42 ± 0.02
100 mM $MgCl_2$ and 0.1 M KCl	0.34 ± 0.02	0.43 ± 0.01
100 mM $MgCl_2$ and 0.6 M KCl	0.10 ± 0.02	0.67 ± 0.06
40 mM $MgCl_2$ and 0.84 M KCl	1.6 ± 0.1	0.40 ± 0.01

[a] All reaction mixtures contain 50 mM Tris-HCl at pH 7.8 and 37 °C.

M^{-1} min^{-1} and 0.8−1.2 min^{-1}, respecgively, from Beebe and Fierke (1994)]. It should be noted here that the dissociation constant for the ribozyme−$tRNA^{Asp}$ substrate (ES) complex is ∼50-fold faster than the dissociation constant of a ribozyme−$tRNA^{Asp}$ product (EP) complex (Beebe & Fierke, 1994). This phenomenon has also been observed for the *Tetrahymena* group I ribozyme in which the dissociation constant of the ES complex is ∼40-fold faster than that of the EP complex (Narlikar et al., 1995).

The effects of Mg^{2+} and K^+ on K_d and k_2 of this $tRNA^{Phe}$ substrate also agree qualitatively with those observed for the $tRNA^{Asp}$ substrate (Table 1; Beebe et al., 1996). The K_d values determined for our $tRNA^{Phe}$ substrate are strongly dependent on the Mg^{2+} concentration. A decrease of Mg^{2+} from 100 to 40 mM resulted in a 16-fold increase in K_d (Table 1). Binding of the $tRNA^{Asp}$ product has been shown to depend on two (or two classes of) Mg^{2+} ions with a midpoint at ∼75 mM (Beebe et al., 1996). At 100 mM $MgCl_2$, the K_d value for the $tRNA^{Phe}$ substrate in the absence of K^+ is 19- and 64-fold higher compared to those at 0.1 and 0.6 M K^+, respectively (Table 1). Binding of the $tRNA^{Asp}$ product to *B. subtilis* P RNA also showed dependence on monovalent ions of similar magnitude (Beebe et al., 1996). A decrease in Mg^{2+} concentration from 100 to 40 mM resulted in only a 1.7-fold decrease in k_2 (Table 1). Within 10−100 mM Mg^{2+}, cleavage of the all-ribo $tRNA^{Asp}$ substrate appears to depend on binding of one Mg^{2+} with $[Mg^{2+}]_{1/2}$ at 36 mM (Beebe et al., 1996). Assuming the same $[Mg^{2+}]_{1/2}$ for cleavage of the $tRNA^{Phe}$ substrate, the increase of k_2 above 40 mM $MgCl_2$ is expected to be less than 2-fold. These results strongly indicate that the K_d and k_2 values obtained from this $tRNA^{Phe}$ substrate accurately reflect the binding affinity and the chemical step of this ribozyme system.

Effects of Single 2′-OH → 2′-H Substitutions in the T Stem−Loop of tRNA. Contributions of individual 2′-OH groups in the T stem−loop to K_d and k_2 of P RNA catalysis were assessed using modified substrates containing two 2′-OH → 2′-H substitutions. One of the 2′-deoxy substitutions was always at the cleavage site, whereas the other was located at the residue of interest. These substrates were made by two ligation reactions of two synthetic oligoribonucleotides at either end of an RNA transcript. The region of interest encompassed the T stem−loop (residues 49−65) plus part of the D loop that interacts with the T loop (residues 18 and 19). Four 2′-OH groups within this region, at residues 54, 57, 61, and 62, have been implicated in direct contacts to P RNA from CPA-DP results (Pan et al., 1995). Of those four, the 2′-OH at residue 62 has been shown to directly contact residue A230 in P RNA (Pan et al., 1995). However, the thermodynamic contribution of this 2′-OH was not determined previously. Table 2 shows the effects of 2′-OH → 2′-H substitutions at these four positions on the K_d and k_2 of the $tRNA^{Phe}$ substrate. In all four cases, the effect on k_2 is small with a maximum of a 2-fold decrease or 0.4 kcal/mol. The predominant effects of these substitutions are on the binding affinity of this substrate, with a maximal increase in K_d of 20-fold or 1.8 kcal/mol. Assuming the free energies of these substitutions are additive, the combined effects of the 2′-OH groups at positions 54, 61, and 62 can be calculated to be ∼2400-fold or 4.7 kcal/mol. Interestingly, all three 2′-OH groups are located within the same minor groove in the tertiary structure of tRNA (Quigley & Rich, 1976). This minor groove is composed in part by two base pairs in the T stem, 53-61 and 52-62, plus the reverse Hoogsteen pair of 54-58 which stacks on the 53-61 pair. The 2′-OH → 2′-H substitution at position 57 shows a much smaller effect, suggesting that the initial implication from the CPA-DP result may be due to other factors (see the Discussion).

Table 2: Effects of Substrate Modification on k_2 and K_d

substrate[a]	K_d (μM)[b]	$\Delta\Delta G$ (kcal/mol)	k_2 (min^{-1})[b]	$\Delta\Delta G$ (kcal/mol)
(d-1)	0.10 ± 0.02	−	0.67 ± 0.06	−
d54	1.6 ± 0.3	1.7	0.71 ± 0.05	0.0
d61	0.74 ± 0.16	1.2	1.01 ± 0.06	−0.3
d62	2.0 ± 0.4	1.8	0.54 ± 0.04	0.1
d57	0.17 ± 0.04	0.3	0.34 ± 0.03	0.4
d56	0.77 ± 0.17	1.2	0.75 ± 0.06	0.0
a19u56	1.1 ± 0.2	1.5	1.1 ± 0.1	−0.3
c19g56	1.9 ± 0.1	1.8	0.70 ± 0.02	0.0

[a] All substrates contain a 2′-deoxynucleotide (d-1) at the cleavage site. [b] Reactions conditions: 50 mM Tris-HCl (pH 7.8), 100 mM $MgCl_2$, and 0.6 M KCl at 37 °C.

CPA-DP results also suggested potential involvement of four other 2′-OHs in this region, residues 53, 55, 56, and 18, in interactions with P RNA. However, due to the lack of activity increase upon removal of the 2′,3′-cyclic phosphate, the effects on cleavage efficiency of the CP isomers may be caused by reasons other than P RNA interaction. Indeed, the CP isomers of residues 53−56 were shown to be misfolded in solution as analyzed by a tRNA folding assay (Pan et al., 1991). Thus, the role of 2′-OH at these positions cannot be unambiguously assessed in the context of their CP isomers. On the other hand, close inspection of the crystal structure of yeast $tRNA^{Phe}$ shows that the 2′-OH groups of residues 53, 54, and 56 do not participate in tertiary folding of tRNA. Hence, single 2′-OH → 2′-H substitutions at these positions are not expected to influence tRNA folding. Inspection of the crystal structure also shows that the 2′-OH groups at positions 55 and 18 are involved in tertiary interactions in the folded tRNA structure. Consequently, 2′-OH → 2′-H substitutions at positions 55 and 18 may result in misfolding. Indeed, a 2′-OH → 2′-H substitution at position 18 produced a misfolded tRNA (data not shown) as assayed by Pb^{2+} cleavage at U17G18 (Brown et al., 1985; Behlen et al., 1990). Therefore, the effects of 2′-OH → 2′-H substitutions at positions 54 and 56 on P RNA catalysis were examined (Table 2). The 2′-OH → 2′-H substitution at position 56 resulted in an ∼8-fold increase in K_d (1.2 kcal/mol) and no effect on k_2.

Effects of Base Mutations in the T Stem−Loop of tRNA. What are the functional roles of conserved bases in the T stem−loop region in mediating interactions with P RNA? A total of four conserved tertiary interactions can be found in this region: G53-C61 (Watson−Crick), U54-A58 (reverse

Table 3: Effects of Ribozyme and Substrate Mutations on k_{cat}/K_m of All-Ribo $tRNA^{Phe}$ Substrates

ribozyme/substrate[a]	relative k_{cat}/K_m
wt/wt	1.00[a]
wt/c19g56	0.035 ± 0.004
wt/c19c56	0.23 ± 0.12
wt/g19g56	0.055 ± 0.006
c130/wt	0.55 ± 0.1
g130/wt	0.078 ± 0.009
u130/wt	0.078 ± 0.009

[a] Reaction conditions: 50 mM Tris-HCl (pH 7.8), 25 mM $MgCl_2$, and 1 M KCl at 37 °C. The k_{cat}/K_m value for the wild-type P RNA with the wild-type $tRNA^{Phe}$ substrate is $(3.0 \pm 0.5) \times 10^7$ M^{-1} min^{-1}.

Hoogsteen), G18-U55, and G19-C56 (tertiary Watson−Crick). The G53-C61 pair also forms a hydrogen bond with the phosphate oxygen of residue 60 and cannot be replaced by other Watson−Crick base pairs without affecting tRNA folding (Sampson et al., 1990; Behlen et al., 1990). Substitutions of U54-A58 and G18-U55 by other natural nucleotides also resulted in misfolded tRNAs. On the other hand, the G19-C56 interaction can be replaced by another Watson−Crick base pair, and the resulting mutant tRNAs fold correctly (Sampson et al., 1990; Behlen et al., 1990). The G19-C56 base pair is located in the corner of the tRNA structure, making its major and minor groove sides accessible for direct contacts with P RNA. The effects of G19-C56 mutations to two other Watson−Crick base pairs are shown in Table 2. In both cases, only a small effect was observed on k_2 of the reaction, whereas the effect on K_d is at least 11-fold or 1.5 kcal/mol. If we assume that the G19-C56 base pair is not disrupted in the P RNA−substrate complex, the specific functional groups in the G19-C56 pair involved in interacting with P RNA can be deduced from the 19-56 mutants. The "minor groove" side of the G19-C56 base pair contains the same set of functional groups (two hydrogen bond acceptors and one donor) upon isosteric replacement by c19-g56. Therefore, the functional groups on the nucleotide base in the minor groove side are unlikely to be involved in direct interactions with P RNA. In contrast, the hydrogen bond donors and acceptors on the "major groove" side have been changed drastically in both a19-u56 and c19-g56 mutations. Therefore, the major groove side of the G19-C56 base pair is likely to mediate interactions with P RNA.

In an attempt to decipher whether G19 or C56 is the more likely candidate for direct interaction, k_{cat}/K_m values for three 19-56 mutants were determined (Table 3). These mutants are not perfect for this purpose since c19-c56 and g19-g56 mutants are misfolded (Sampson et al., 1990; Behlen et al., 1990). The interpretation of the k_{cat}/K_m values is based on the assumption that the misfolded mutants do not specifically have non-native interactions with P RNA. For the c19-g56 mutant, the k_{cat}/K_m decreased by 28-fold. The catalytic efficiency can be improved to within 4-fold of the wild-type value with the c19-c56 mutant, but not with the g19-g56 mutant. The simplest explanation is that the direct ribozyme−substrate interaction is more likely to involve C56 than G19. Assuming further that the G19-C56 Watson−Crick base pairing is to be maintained, then the 4-amino group of C56 is the most likely candidate for this interaction.

Combining the base mutation data with the result from 2′-OH → 2′-H modification at 56, both the major groove and the minor groove sides of the G19-C56 base pair appear to be contacted by P RNA. These contacts are likely to involve the 4-amino group of C56 in the major groove side and the 2′-OH of position 56 in the minor groove side.

Effects of P RNA Mutations on the K_d and k_2 of the Cleavage Reaction. The putative four-way junction, the P7−P11 region in folding domain I, in P RNA has been postulated to directly contact the T stem−loop in tRNA (Harris et al., 1994; Pan et al., 1995). Chemical modification with dimethyl sulfate and kethoxal has shown that two residues, A130 and A230 which are located within or in the immediate proximity of this four-way junction, may directly contact tRNA (LaGrandeur et al., 1994). Previous experiments have suggested that the N^1 of A230 interacts with the 2′-OH of residue 62 in tRNA (Pan et al., 1995). An A → G mutation changing the N^1 position from a hydrogen bond acceptor to a donor reduced the k_{cat}/K_m of an all-ribo $tRNA^{Phe}$ substrate by ∼170-fold (Pan et al., 1995). This A230G mutation (g230) exerted a 240-fold reduction on K_d and a 6-fold reduction on k_2 of the $tRNA^{Phe}$ substrate with a 2′-OH → 2′-H at the cleavage site (Table 4), much more than the largest reduction by any single substitution in the tRNA substrate. This result suggests that this mutation is more disruptive than the loss of a single interaction with the 2′-OH at residue 62. For example, this mutation may disrupt other tertiary interactions indirectly due to the presence of different functional groups on G relative to A. Mutation of A130 to G (g130) also exerted an appreciable effect on K_d of the $tRNA^{Phe}$ substrate (Table 4). The g130 and the g230 mutants are properly folded at identical Mg^{2+} concentrations compared to folding of the wild-type P RNA as analyzed by the Fe(II)−EDTA protection assay [data not shown and Pan (1995) and Pan et al. (1995)]. Thus, the kinetic data of the g130 mutant suggest that A130 is involved in direct contact with tRNA substrate, consistent with the chemical modification data.

As a further control to ensure that the kinetics of these P RNA mutants reflect intermolecular interaction, effects of an A179G mutant (g179) on K_d and k_2 were determined (Table 4). A179 is located in J10/11 which is a part of the putative four-way junction, P7−P11. A179 is phylogenetically conserved (Haas et al., 1994) but shows no protection from chemical modification upon tRNA binding (LaGrandeur et al., 1994). Indeed, both K_d and k_2 values for the g179 mutant are within 1.5-fold of those for the wild-type P RNA, indicating that A179 is not involved in substrate binding.

What is the possible nature of A130−tRNA interaction? The phylogeny of bacterial P RNAs (from a total of 57 sequences in the RNase P data base; Brown, 1996) shows that adenosine and cytosine occur 40 and 9 times at the corresponding position of A130 in *B. subtilis* P RNA. Since A and C have a similar hydrogen bonding face with the N^1 and 6-NH_2 of A compared to the N^3 and 4-NH_2 of C, these two groups may be crucial for the intermolecular interaction. A130 is protected from dimethyl sulfate modification (which modified N^1 of A) upon substrate binding. The A130C mutant (c130) is only ∼2-fold less efficient in k_{cat}/K_m compared to the wild-type P RNA (Table 3). When this hydrogen bonding face is changed in the A130G and A130U mutants, the catalytic efficiency decreased by more than 12-fold (Table 3), consistent with the notion that either N^1 or 6-NH_2 of A130 or both interact with the tRNA substrate.

The A130G mutant was constructed with the intent that the switches of the hydrogen bond donor and acceptor at

Table 4: Effects of Ribozyme Mutations on k_2 and K_d

ribozyme/substrate[a]	K_d (μM)[b]	$\Delta\Delta G$ (kcal/mol)[c,d]	k_2 (min^{-1})[b]	$\Delta\Delta G$ (kcal/mol)[c,d]
wt	0.10 ± 0.02	−	0.67 ± 0.06	−
g230	24 ± 3	3.4	0.11 ± 0.01	1.1
g179	0.14 ± 0.01	0.2	0.92 ± 003	−0.2
g130	2.7 ± 0.4	2.0 (−)	0.33 ± 0.02	0.4 (−)
g130/d56	5.2 ± 1.6	(0.4) [1.2]	0.10 ± 0.01	(0.7) [0.0]
g130/a19u56	15 ± 3	(1.1) [1.5]	0.18 ± 0.02	(0.4) [−0.3]
g130/c19g56	17 ± 4	(1.1) [1.8]	0.04 ± 0.006	(1.2) [0.0]

[a] All substrates contain a 2′-deoxynucleotide (d-1) at the cleavage site. [b] Reactions conditions: 50 mM Tris-HCl (pH 7.8), 100 mM $MgCl_2$, and 0.6 M KCl at 37 °C. [c] $\Delta\Delta G$ values in parentheses are relative to the reaction by g130 ribozyme with d-1 substrate ($K_d = 2.7 \pm 0.4$ μM, $k_2 = 0.33 \pm 0.02$ min^{-1}). [d] $\Delta\Delta G$ values in brackets are the $\Delta\Delta G$ values for the same modified substrates determined with the wild-type P RNA (from Table 2).

positions N^1 and N^6 of A to the hydrogen bond acceptor and donor in G may result in a compensatory change with a modified tRNA substrate. This possibility was tested with substrates containing base mutations of the G19-C56 tertiary interaction (Table 4). The effects on K_d and k_2 for g130/a19u56 and for g130/c19g56 are more detrimental compared to those of the g130 reaction with the wild-type substrate. Compared to the calculated cumulative values (the $\Delta\Delta G$ values in parentheses compared to those in brackets in Table 4), however, the K_d values show improvements of 0.4−0.7 kcal/mol, whereas the k_2 values show simultaneous losses of 0.7−1.2 kcal/mol. These results can be explained by the occurrence of a non-native interaction in the g130/19-56 mutant substrate complexes (for detailed descriptions, see the Discussion).

If the N^1 position of A130 is involved in hydrogen bonding to a 2′-OH group in tRNA, its mutation to a G would result in the loss of this hydrogen bond. Therefore, the A130G mutant may be insensitive to a 2′-OH → 2′-H substitution in tRNA at the specific position involved in this interaction (Pyle et al., 1992). It was difficult to accurately determine the K_d for the g130/d54 complex which has increased to >20 μM. As for the g130/d56 combination, the effects are similar to those observed for the g130/a19u56 and g130/c19g56 reactions (Table 4). Thus, it is not possible to conclude from these data whether the 2′-OH groups of residues 54 and 56 in the tRNA substrate interact with A130 in P RNA.

DISCUSSION

We have described the effect of single-atom substitutions in the T stem−loop region of a tRNA substrate on the binding and chemical step of P RNA catalysis. This was made possible by using a $tRNA^{Phe}$ substrate with a 2′-deoxy residue at the cleavage site. Several lines of evidence indicate that this modified substrate accurately reflects the properties of the all-ribo substrate. (1) The K_d value for the modified substrate (0.10 μM) is identical to that calculated from microscopic rate constants [0.11 μM, from Beebe and Fierke (1994)]. (2) The k_2 value is logarithmically linear with pH with a slope of 1.1. Such a pH dependence on the chemical step has also been suggested for the all-ribo substrate (Smith & Pace, 1993; Beebe & Fierke, 1994). (3) The rate reduction upon substituting the 2′-OH → 2′-H at the cleavage site is ∼540-fold (from 360 to 0.67 min^{-1}). This value is comparable to those observed for the *Tetrahymena* group I ribozyme [∼270-fold for the chemical step in the absence of G and 590-fold for k_{cat}/K_m in the presence of G, from Herschlag et al. (1993)]. Thus, the $\Delta\Delta G$ values observed for individual 2′-OH → 2′-H substitutions and G19-C56 mutations in the T stem−loop region provide a detailed picture of the intermolecular tertiary interactions between the P RNA and its tRNA substrate.

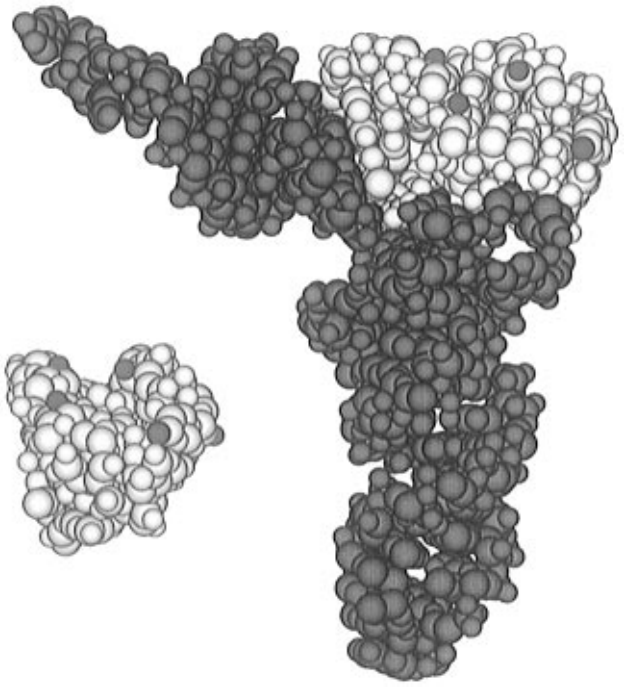

FIGURE 3: Location of the five functional groups involved in direct interactions with *B. subtilis* P RNA in the tertiary structure of $tRNA^{Phe}$. The T stem−loop residues (49−65) and nucleotides 18 and 19 in the D loop are shown in white, whereas the rest of the tRNA is shown in gray. The 2′-OHs of residues 54, 61, and 62 and the 4-amino of C56 are shown in red. The 2′-OH of residue 56 and the cleavage site phosphate are on the other side of this view and cannot be seen from this angle. (Insert) The region shown in white rotated by ∼30° along the *y*-axis and by ∼10° along the *x*-axis to allow a better view of the "tertiary groove" and the location of the 2′-OH of residue 56.

At least five functional groups in the T stem−loop region are directly involved in binding to P RNA (Figure 3). These five groups include four 2′-OHs at residues 54, 56, 61, and 62 and possibly the 4-amino group of residue C56. They can be further divided into two groups. The 2′-OHs of residues 54, 61, and 62 are located in the same minor groove brought together in the tertiary structure of tRNA. This minor groove is formed by the Watson−Crick base pairs of G53-C61 and U52-A62 in the T stem and by the reverse Hoogsteen pair of U54-A58 which stacks on the G53-C61 base pair. Due to the participation of the tertiary U54-A58 interaction, the geometry of these three 2′-OHs is unlike those in a standard A-form helix. The distance between 2′-OH-

(61) and 2′-OH(62) is 6.6 Å, whereas the distance between 2′-OH(54) and its nearest neighbor, 2′-OH(61), is 8.4 Å. If we assume that the free energies of these interactions are additive, these three 2′-OHs contribute a total of 4.7 kcal/mol in substrate binding, but only −0.2 kcal/mol in the chemical step. The average $\Delta\Delta G$ values for binding (1.6 kcal/mol) are consistent with tertiary interactions involving a single hydrogen bond with 2′-OH groups.

The second group in the T stem−loop region involved in P RNA recognition centers around residue C56 (Figure 3). This nucleotide is 100% conserved in all cytoplasmic tRNAs, and it forms a tertiary Watson−Crick base pair with another 100% conserved nucleotide, G19. The G19-C56 tertiary base pair is situated at the edge of the tRNA structure; both the major groove and the minor groove sides are accessible for intermolecular interaction. Our data suggest that both groove sides are contacted by the P RNA. The maximum $\Delta\Delta G$ value for the possible involvement of the 4-amino group of C56 is likely to be that for the a19-u56 mutant (Table 2), since this mutant changes the 4-amino to 4-keto without any steric complications. The sum of free energies for both interactions is 2.7 kcal/mol for substrate binding and −0.3 kcal/mol for the chemical step.

These two groups of interactions are connected through the tertiary structure of tRNA. The groove starting with the three 2′-OHs can be extended to include the 4-amino of C56 at a distance of 11.6 Å to the 2′-OH of residue 54 (Figure 3). This extension is only possible because of the tertiary folding of tRNA. In a sense, the P RNA binding surface in tRNA can be described as a "tertiary groove" (to contrast with major or minor grooves in a standard nucleic acid helix). This groove is aligned with hydrogen bonding groups beginning with the 2′-OH of residue 62 which is still a part of the standard A-form minor groove of the T stem. The 2′-OH(62) is followed by the 2′-OH(61) through an A-form minor groove, then through a non-A-form minor groove to 2′-OH(54), and then through an extension to the 4-amino of C56. Assuming additivity, the total free energy contribution of all five interactions on binding is 7.4 kcal/mol at 37 °C (a factor of 10^5). On the other hand, the contribution to the chemical step is only −0.5 kcal/mol at 37 °C (∼2-fold). Thus, the T stem−loop recognition by P RNA is a major determining factor for specific binding of a tRNA substrate but has virtually no effect on the chemistry of P RNA catalysis.

How does the recognition of the T stem−loop region by P RNA compare to specific RNA binding by other macromolecules? The active site of the *Tetrahymena* group I ribozyme recognizes an RNA helix with an essential G-U wobble pair at the cleavage site (Strobel & Cech, 1995). Three 2′-hydroxyl groups and the 2-amino group of G in the G-U wobble pair are involved in direct contacts, contributing up to a total of 8.3 kcal/mol in binding. The alanyl aminoacyl-tRNA synthetase also recognizes a set of 2′-OH groups plus the 2-amino group of G in the G3-U70 wobble pair in the acceptor stem of $tRNA^{Ala}$ (Musier-Forsyth et al., 1991; Musier-Forsyth & Schimmel, 1992). The MS2 coat protein interacts with three adenosines in a hairpin loop with a bulge (Valegard et al., 1994). The U1A protein binds to seven contiguous nucleotides in a hairpin loop (Oubridge et al., 1994). In the cases of MS2 coat protein and the U1A protein, however, the protein−RNA interactions rely largely on the functional groups in the nucleotide bases. Thus, an RNA can be specifically bound in at least two ways through non-Watson−Crick interactions. To recognize a highly structured RNA as in the cases of helix P1 by *Tetrahymena* group I intron and the acceptor stem of a tRNA by the alanyl tRNA-synthetase, 2′-OH groups and particular functional groups on nucleotide bases in specific structural contexts are utilized. Binding of MS2 and U1A protein to their corresponding RNA also requires the presence of an RNA structure, e.g. a hairpin loop. The nucleotide bases needed for binding, however, are not involved in forming this structure. Recognition of a tRNA substrate by P RNA is more like the operational mode of the *Tetrahymena* group I ribozyme and the alanyl tRNA-synthetase in that particular functional groups embedded in a specific RNA structure are used. The differences are in how these functional groups are positioned: either in a tertiary groove as in the case of tRNA−P RNA or in the minor groove of an A-form helix as in the other cases.

Several lines of evidence suggest that the T stem−loop binding site in *B. subtilis* P RNA is located mainly in the folding domain I [residues 86−239, from Pan (1995) and Loria and Pan (1996)]. (1) Residue A230 in *B. subtilis* P RNA has been shown to interact with the 2′-OH of residue 62 (Pan et al., 1995). (2) An *in vitro* selected RNA substrate binds to a P RNA variant lacking the entire folding domain I (Pan & Jakacka, 1996). This RNA substrate contains an acceptor stem-like structure but lacks the T stem−loop-like structure of a tRNA. (3) Aryl azide cross-linkers with an ∼9 Å linker arm positioned at nucleotides 53 and 64 in tRNA primarily cross-link to residues of the corresponding folding domain I in *E. coli* P RNA (Nolan et al., 1993; Harris et al., 1994). The highly ordered structure of this folding domain in part hinders identification of nucleotide bases that are involved in direct contacts with tRNA by chemical modification. Only ∼20 out of ∼140 nucleotides in this folding domain are accessible at 37 °C to probing by chemical modification in the presence and absence of tRNA. Nevertheless, three nucleotide bases in *B. subtilis* P RNA, A130, G220, and A230, were shown to make direct contact with tRNA (L. Odell and T. Pan, unpublished results). Both A130 and A230 were also identified as contact sites at 0 °C (LaGrandeur et al., 1994). Their phylogenetically equivalent residues in *E. coli* P RNA (A118, A180, and A233) and in *Chromatium vinosum* P RNA (A99, A158, and A210) have also been shown to potentially contact tRNA (LaGrandeur et al., 1994).

Both phylogenetic and biochemical data have indicated the involvement of A230 and A130 in contacting tRNA. Out of 57 sequences in the bacterial P RNA data base (Brown, 1996), the residue corresponding to A230 in *B. subtilis* P RNA occurs 55 times. As mentioned earlier, A230 has been shown to interact with the 2′-OH of residue 62 in the T stem of tRNA. The free energy of this interaction measured with a 2′-OH → 2′-H substitution at residue 62 is 1.8 kcal/mol for binding with no effect on chemistry (Table 2). The A230G mutant caused a further reduction of 1.6 kcal/mol in tRNA binding, suggesting that a G at this position resulted in the loss of an interaction elsewhere. This misalignment of the tRNA substrate with the A230G mutant is also suggested by a 1.1 kcal/mol reduction in k_2 (Table 4). The residue identity at the position corresponding to nucleotide 130 in *B. subtilis* P RNA is either an A (40 out of 57 times) or a C (9 out of 57). Since A and C can have the same

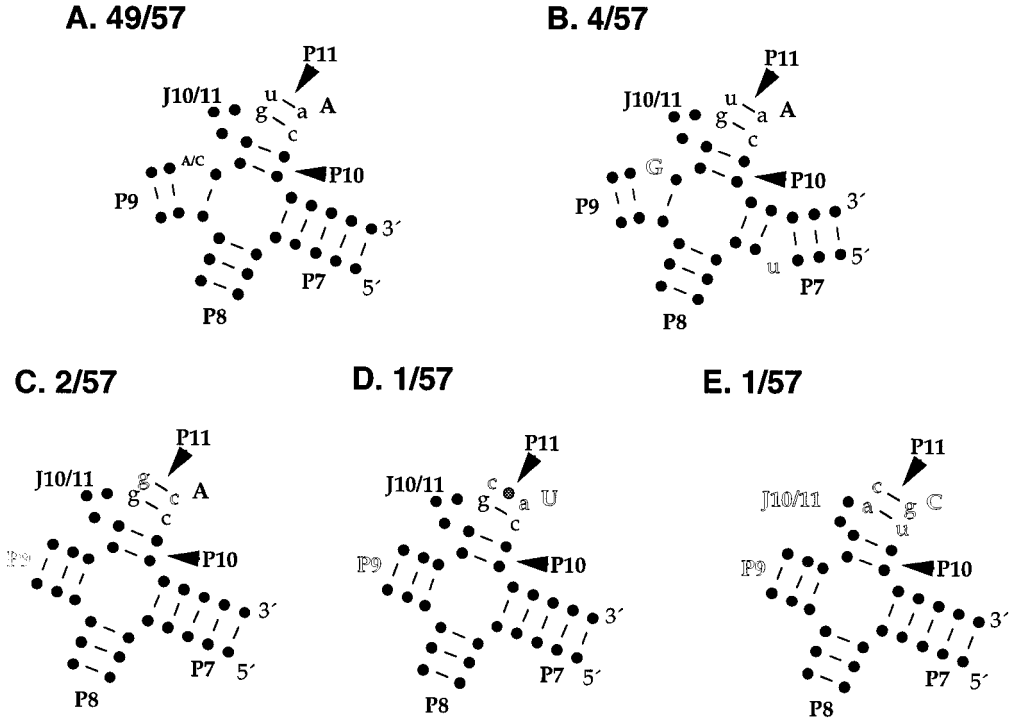

FIGURE 4: Nucleotide composition and the secondary structure of the putative four-way junction, P7−P11 region, in bacterial P RNAs [from the P RNA data base; see Brown (1996)]. (A) The majority (49 out of 57 P RNA sequences) contains an A/C and an A at the corresponding positions of A130 and A230 in the *B. subtilis* P RNA. Nucleotide 220 in *B. subtilis* P RNA and its corresponding nucleotide (not pictured) are purines in all but the cyanobacterial P RNAs (panel B). The base pair in P11 immediately following A230 is >95% U-A. (B) P RNAs from cyanobacteria have simultaneous changes at 130 (A/C → G) and 220 (A/G → C) and an extra bulged nucleotide in P7. (C) P RNAs from *Thermotogales* have an uninterrupted helix P9 (=deletion of nucleotide 130) and a U-A → G-C base pair in P11. (D) P RNA from *D. desulfuricans* has a nucleotide 130 deletion (A230 → U) and a C·A mismatch at P11. (E) P RNA from *B. thetaiotaomicron* has a nucleotide 130 deletion (230 → C) and a C-G base pair in P11. The J10/11 region also has one nucleotide less than that in the other P RNAs.

hydrogen bonding face, this suggests that the intermolecular interaction would involve either N^1 or 6-NH_2 of A, consistent with the chemical modification data. The A130G mutant caused a reduction of 2.0 kcal/mol in tRNA binding and a decrease of 0.4 kcal/mol in k_2. The 2.0 kcal/mol in binding is likely the maximal contribution of the interaction involving A130. The residue identity at the position corresponding to nucleotide 220 in *B. subtilis* P RNA is most commonly an A (35 out of 57 times) or a G (18 out of 57 times). The requirement of purine at this position suggests its role as a hydrogen bond acceptor using either N^3 or N^7 in tRNA binding.

It is interesting to discuss the few cases in which the phylogeny of the corresponding nucleotides 130, 220, and 230 differs from that of the majority (Figure 4). When nucleotide 230 is not an A (2 out of 57, one U and one C), nucleotide 130 is deleted. These two P RNAs (*Desulfovibrio desulfuricans* and *Bacteroides thetaiotaomicron*) also have unusual changes in the helix P11 and/or its adjacent loop, J10/11 (Figure 4D,E). The two other P RNAs with nucleotide 130 deletion are from *Thermotogales*, the deepest branch in the eubacterial phylogenetic tree. The P11 sequence for *Thermotoga* P RNAs differs from the other bacterial P RNAs in that the adjacent base pair of A230 is G-C rather than U-A (Figure 4C). The most divergent sequence is found in cyanobacteria in which nucleotide 130 is a G and nucleotide 220 is a C. It differs from other bacterial P RNAs in that helix P7 contains an extra one-nucleotide bulge (Figure 4B). Thus, all these changes in the nucleotide identity of 130 and 220 are accompanied by unusual changes in the structure of the putative four-way junction, P7−P11.

Although the precise functional group in tRNA that interacts with A130 remains elusive, our kinetic data give clues to where A130 may be located in the P RNA−tRNA complex. The three modifications at nucleotide 56 combined with g130 resulted in nonadditive K_d and k_2 values. Relative to the added values, there is a consistent improvement in K_d by 0.4−0.8 kcal/mol and a simultaneous decrease in k_2 by 0.7−1.2 kcal/mol. The opposite effects on K_d and k_2 of modified residue 56 substrates may be explained by the occurrence of a non-native ribozyme−substrate interaction with the A130G mutant. This interaction can give rise to better binding but misaligns the substrate in the active site of P RNA, resulting in a decrease of the chemical step. Since this non-native interaction is more prevalent upon modifications of both A130 and residue 56, this interdependency may suggest their physical proximity. A re-examination of the CPA-DP data suggests that such a non-native interaction involving the circularly permuted isomer of residue 57 may have produced the "false positive" result for this position. CPA was carried out under k_{cat}/K_m conditions in which the substrate binding, but not the chemical step, was a significant factor (Pan et al., 1995). Tertiary folding of this CP isomer does not appear to be affected (Pan et al., 1991).

It is difficult to compare our results to the structural models of the *E. coli* P RNA which are not modeled at the atomic resolution. The *E. coli* P RNA also contains the phylogenetically conserved A130 (=A118) in P9, A230 (=A233) immediately 5′ to P11, and G220 (=A180) in J12/13 (Haas

et al., 1994). The putative four-way junction of P7−P11 is modeled by Pace and co-workers to be proximal to the T stem−loop region (Harris et al., 1994). This model is consistent with the previously found intermolecular A230−2′-OH(62) interaction (Pan et al., 1995). This putative four-way junction was also modeled to be close to the T stem−loop in the Westhof−Altman model (Westhof et al., 1996). In that model, however, one of the major components of T stem−loop recognition involves the GA_3 tetraloop in loop L9 of the *E. coli* P RNA. The sequence of loop L9 in *B. subtilis* P RNA is 5′-UUAG, and the length of P9 differs from that of the *E. coli* P RNA. Neither the sequence of L9 nor the length of P9 are conserved among the subclass of bacterial P RNAs containing secondary structures similar to *B. subtilis* P RNA. Therefore, the T stem−loop recognition is unlikely to involve loop L9 of *B. subtilis* P RNA.

The five functional groups in the T stem−loop region involved in direct P RNA contact are likely to represent a subset of all intermolecular interactions within this region. For example, several nonbridging phosphate oxygens in this region have also been suggested to interact with P RNA (Gaur et al., 1996). These phosphate oxygens may function as hydrogen bond acceptors or as ligands for the Mg^{2+} binding sites in the P RNA−tRNA complex (Beebe et al., 1996). Nevertheless, the major feature of T stem−loop recognition by P RNA appears to be the functional groups positioned in a groove-like structure dictated by the tertiary structure of tRNA. The structural uniqueness of a tertiary groove may be commonly applied for recognition of highly structured RNAs.

ACKNOWLEDGMENT

We thank Dr. Joe Piccirilli for his insightful discussions and comments. We also thank the reviewers for helpful suggestions on the manuscript.

REFERENCES

Altman, S., Kirsebom, L., & Talbot, S. (1993) *FASEB J. 7,* 7−14.
Beebe, J. A., & Fierke, C. A. (1994) *Biochemistry 33,* 10294−10304.
Beebe, J. A., Kurz, J. C., & Fierke, C. A. (1996) *Biochemistry 35,* 10493−10505.
Behlen, L. S., Sampson, J. R., DiRenzo, A. B., & Uhlenbeck, O. C. (1990) *Biochemistry 29,* 2515−2523.
Brown, J. W. (1996) *Nucleic Acids Res. 24,* 236−238.
Brown, R. S., Dewan, J. C., & Klug, A. (1985) *Biochemistry 24,* 4785−4801.
Cech, T. R. (1993) in *The RNA World* (Gesteland, R., & Atkins, J., Eds.) pp 239−269, Cold Spring Harbor Laboratory Press, Plainview, NY.
Doudna, J. A., & Szostak, J. W. (1989) *Nature 339,* 519−522.
Doudna, J. A., & Cech T. R. (1995) *RNA 1,* 36−45.
Gaur, R. K., Hanne, A., Conrad, F., Kahle, D., & Krupp, G. (1996) *RNA 2,* 674−681.
Guerrier-Takada, C., Gardiner, K., Marsh, T., Pace, N., & Altman, S. (1983) *Cell 35,* 849−857.
Haas, E. S., Morse, D. P., Brown, J. W., Schmidt, F. J., & Pace, N. R. (1991) *Science 254,* 853−856.
Harris, M. E., Nolan, J. M., Malhotra, A., Brown, J. W., Harvey, S. C., & Pace, N. R. (1994) *EMBO J. 13,* 3953−3963.
Herschlag, D., Eckstein, F., & Cech, T. (1993) *Biochemistry 32,* 8312−8321.
Kahle, D., Wehmeyer, U., & Krupp, G. (1990) *EMBO J. 9,* 1929−1937.
Kirsebom, L. A., & Svard, S. G. (1994) *EMBO J. 13,* 4870−4876.
LaGrandeur, T. E., Huttenhofer, A., Noller, H. F., & Pace, N. R. (1994) *EMBO J. 13,* 3945−3952.
Loria, A., & Pan, T. (1996) *RNA 2,* 551−563.
McClain, W. H., Guerrier-Takada, C., & Altman, S. (1987) *Science 238,* 527−530.
Milligan, J. F., Groebe, D. R., Witherell, G. W., & Uhlenbeck, O. C. (1987) *Nucleic Acids Res. 15,* 8783−8798.
Moore, M. J., & Sharp, P. A. (1992) *Science 256,* 992−997.
Musier-Forsyth, K., & Schimmel, P. (1992) *Nature 357,* 513−515.
Musier-Forsyth, K., Usman, N., Scaringe, S., Doudna, J., Green R., & Schimmel, P. (1991) *Science 253,* 784−786.
Narlikar, G. J., Gopalakrishnan, V., McConnell, T. S., Usman, N., & Herschlag, D. (1995) *Proc. Natl. Acad. Sci. U.S.A. 92,* 3668−3672.
Nolan, J. M., Burke, D. H., & Pace, N. R. (1993) *Science 261,* 762−765.
Oh, B.-K., & Pace, N. R. (1994) *Nucleic Acids Res. 22,* 4087−4094.
Oubridge, C., Ito, N., Evans, P. R., Teo, C.-H., & Nagai, K. (1994) *Nature 372,* 432−438.
Pace, N. R., & Brown, J. W. (1995) *J. Bacteriol. 177,* 1919−1928.
Pan, T. (1995) *Biochemistry 34,* 902−909.
Pan, T., & Jakacka, M. (1996) *EMBO J. 15,* 2249−2255.
Pan, T., Gutell, R. R., & Uhlenbeck, O. C. (1991) *Science 254,* 1361−1364.
Pan, T., Loria, A., & Zhong, K. (1995) *Proc. Natl. Acad. Sci. U.S.A. 92,* 12510−12514.
Pyle, A. M., Murphy, F. L., & Cech, T. R. (1992) *Nature 358,* 123−128.
Quigley, G., & Rich, A. (1976) *Science 194,* 796−806.
Sampson, J. R., DiRenzo, A. B., Behlen, L. S., & Uhlenbeck, O. C. (1990) *Biochemistry 29,* 2523−2532.
Scaringe, S. (1996) Ph.D. Thesis, University of Colorado at Boulder, Boulder, CO.
Smith, D., & Pace, N. R. (1993) *Biochemistry 32,* 5273−5281.
Strobel, S. A., & Cech, T. R. (1993) *Biochemistry 32,* 13593−13604.
Strobel, S. A., & Cech, T. R. (1995) *Science 267,* 675−679.
Thurlow, D. L., Shilowski, D., & Marsh, T. L. (1991) *Nucleic Acids Res. 19,* 885−891.
Valegard, K., Murray, J. B., Stockley, P. G., Stonehouse, N. J., & Liljas, L. (1994) *Nature 371,* 623−626.
Westhof, E., & Altman, S. (1994) *Proc. Natl. Acad. Sci. U.S.A. 91,* 5133−5137.
Westhof, E., Wesolowski, D., & Altman, S. (1996) *J. Mol. Biol. 258,* 600−613.

BI970115O